

2013

An Assessment of the Ability of the TFM Approach to Predict Gas Mixing in a Pseudo-2D Bubbling Fluidized Bed

Abdelghafour Zaabout
SINTEF Materials and Chemistry, Norway

Schalk Cloete
Norwegian University of Science and Technology (NTNU), Norway

Martin van Sint Annaland
Technical University of Eindhoven (TU/e), Netherlands

Fausto Gallucci
Technical University of Eindhoven (TU/e), Netherlands

Shahriar AMini
SINTEF Materials and Chemistry, Norway

Follow this and additional works at: http://dc.engconfintl.org/fluidization_xiv

 Part of the [Chemical Engineering Commons](#)

Recommended Citation

Abdelghafour Zaabout, Schalk Cloete, Martin van Sint Annaland, Fausto Gallucci, and Shahriar AMini, "An Assessment of the Ability of the TFM Approach to Predict Gas Mixing in a Pseudo-2D Bubbling Fluidized Bed" in "The 14th International Conference on Fluidization – From Fundamentals to Products", J.A.M. Kuipers, Eindhoven University of Technology R.F. Mudde, Delft University of Technology J.R. van Ommen, Delft University of Technology N.G. Deen, Eindhoven University of Technology Eds, ECI Symposium Series, (2013). http://dc.engconfintl.org/fluidization_xiv/134

An assessment of the ability of the TFM approach to predict gas mixing in a pseudo-2D bubbling fluidized bed

Abdelghafour Zaabout^{1,3}, Schalk Cloete², Martin van Sint Annaland³, Fausto Gallucci³
& Shahriar AMini¹

1) SINTEF Materials and Chemistry, Norway

2) Norwegian University of Science and Technology (NTNU), Norway

3) Technical University of Eindhoven (TU/e), the Netherlands;

E: abdelghafour.zaabout@gmail.com

ABSTRACT

2D and 3D simulations of gas species diffusion in a pseudo-2D bubbling fluidized bed were carried out and compared to experimental measurements. Tracer gas concentration and solids velocity profiles measured throughout the bed showed great deviations of the 2D simulations due to negligence of the friction on the large front and back walls of the pseudo-2D unit and the inability to resolve gas species gradients across the thickness of the bed. 3D simulations circumvent these limitations and result in much more reasonable comparisons with experimental data. A clear lack of gas species diffusion was observed, however, and this was attributed to the negligence of particle-induced diffusion of gas species within the bed. Further work is recommended to investigate the modelling of particle-induced gas species diffusion in fluidized bed reactors.

INTRODUCTION

Numerical modelling of fluidized beds has enjoyed considerable research attention over the past few decades. The most popular approach is known as the Two Fluid model (TFM) which simulates the gas and solid phases in the fluidized bed as interpenetrating continua (fluids). The TFM usually employs a set of closure laws known as the Kinetic Theory of Granular Flows (KTGF) (1, 2) to modify the internal stresses of the fluid representing the solids phase, thereby making it behave more like a granular medium.

Although considerable room for further improvement exists, the TFM closed by the KTGF has been shown to give adequate predictions of fluidized bed hydrodynamics (e.g. (3)). Thus, research efforts have been extended to incorporate chemical kinetics and simulate complete fluidized bed reactors. The additional physics included in this extension significantly increases the complexity of the problem due to the tight coupling between reactor hydrodynamics, heat transfer, species transfer and kinetics. More research is therefore required to build the understanding necessary for carrying out sufficiently accurate fluidized bed reactor simulations.

One of the open questions in the modelling of reactive fluidized bed systems is the species transfer in the emulsion phase. A recent study on gas dispersion in a packed bed (4) concluded that packed particles have a significant diffusive influence on the transport of a concentrated tracer gas. The physical interpretation of the phenomenon is shown in Figure 1.

This paper will investigate whether this or other diffusive phenomena (e.g. particle induced turbulence) are also significant in fluidized bed reactors by comparing

simulations with the standard TFM approach (without any special treatment of the gas diffusion) to dedicated experiments completed in a pseudo-2D fluidized bed unit. The results will give a clear indication about whether additional work is necessary to model particle-induced gas species diffusion in fluidized bed reactors.

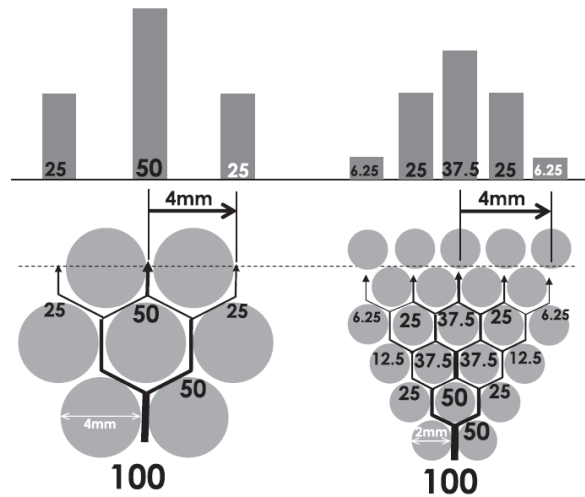


Figure 1: Particle-induced gas species diffusion as portrayed in (4). The presence of particles causes a concentrated tracer gas to repeatedly branch out, thereby experiencing greatly enhanced diffusion.

EXPERIMENTS

Experimental set up

The experimental setup (Figure 2) consisted of a pseudo-2D fluidized bed column with a height of 1.5 m, a width of 0.3 m and a depth of 0.015 m. A porous plate with 40 μm average pore size and 3 mm thickness was used as the gas distributor. Mass flow controllers were used to control the gas inlet flow rate and the column was equipped with an expanding metallic freeboard at the top in order to prevent elutriation of fine particles at higher flow rates (see [ref] for more details about the experimental set up). The setup has been used for both particle image velocimetry measurements and gas injection-extraction measurements.

Spherical glass beads with a density of 2500 kg/m^3 were used as the bed medium. A narrow particle size distribution in the range of 400-600 μm was used ($D_{10} = 430 \mu\text{m}$, $D_{50} = 478 \mu\text{m}$ & $D_{90} = 526 \mu\text{m}$). Humidified air at ambient temperature was used as the fluidizing gas.

A 5 mm inner diameter tube was used as the probe for gas injection from a port on the back plate located at the centre of the column and 5.5 cm above the distributor. CO_2 was injected as the tracer gas at a rate corresponding to 3% of the fluidization flowrate. The same probe was used for gas extraction to be sent to a Micro GC for gas sampling through a capillary tube. Three samples were analyzed for each measurement point.

A high speed CCD camera (Lavision model Image Pro HS4M) was used to film the bed from the front for the purpose of determining the particle velocity field based on PIV/DIA (discussed further below). Lighting was supplied by four LED lamps.

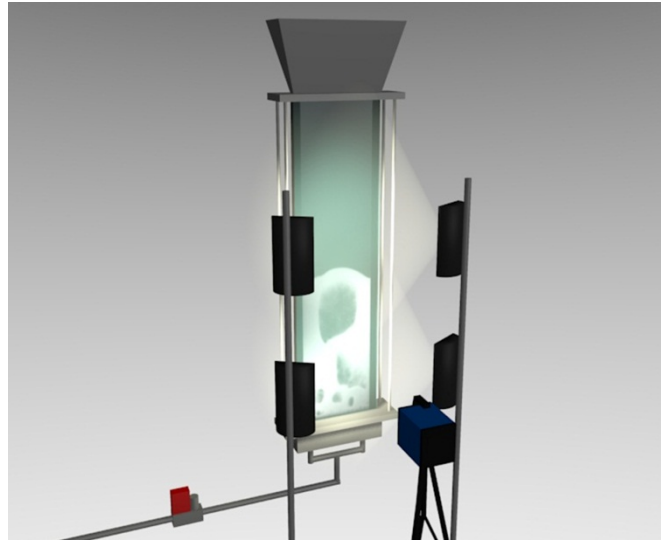


Figure 2: Schematic representation of the experimental set up.

Particle image velocimetry

PIV is a non-invasive optical measurement technique that determines the particle velocity from two images recorded in short succession. The two images are analysed by first dividing each image into $N \times N$ interrogation areas and then applying a cross correlation to determine the average particle displacement in each interrogation area. The measurement procedure and the requirements for good statistics are described in Cloete et al. 2013 (5)

SIMULATIONS

Simulations were carried out both on a 2D planar geometry and on a full 3D geometry using the standard TFM closed by a fairly standard version of the KTGF.

Model equations

Conservation equations are solved for each of the two phases present in the simulation. The continuity equations for the gas and solids phases are given below:

$$\frac{\partial}{\partial t}(\alpha_g \rho_g) + \nabla \cdot (\alpha_g \rho_g \vec{v}_g) = 0 \quad \text{Eq. 1}$$

$$\frac{\partial}{\partial t}(\alpha_s \rho_s) + \nabla \cdot (\alpha_s \rho_s \vec{v}_s) = 0 \quad \text{Eq. 2}$$

Momentum conservation for the gas phase is written as

$$\frac{\partial}{\partial t}(\alpha_g \rho_g \vec{v}_g) + \nabla \cdot (\alpha_g \rho_g \vec{v}_g \vec{v}_g) = -\alpha_g \nabla p + \nabla \cdot \bar{\bar{\tau}}_g + \alpha_g \rho_g \bar{\bar{g}} + K_{sg} (\vec{v}_s - \vec{v}_g) \quad \text{Eq. 3}$$

And for the solids as

$$\frac{\partial}{\partial t}(\alpha_s \rho_s \bar{v}_s) + \nabla \cdot (\alpha_s \rho_s \bar{v}_s \bar{v}_s) = -\alpha_s \nabla p - \nabla p_s + \nabla \cdot \bar{\tau}_s + \alpha_s \rho_s \bar{g} + K_{gs} (\bar{v}_g - \bar{v}_s) \quad \text{Eq. 4}$$

The inter-phase momentum exchange coefficient ($K_{gs} = K_{sg}$) was modelled according to the formulation of Syamlal and O'Brien (6).

Solids phase stresses were determined according to the KTGF analogy. The conservation equation for granular temperature is given below:

$$\frac{3}{2} \left[\frac{\partial}{\partial t} (\alpha_s \rho_s \Theta_s) + \nabla \cdot (\alpha_s \rho_s \bar{v}_s \Theta_s) \right] = \left(-p_s \bar{I} + \bar{\tau}_s \right) : \nabla \bar{v}_s + \nabla \cdot (k_{\Theta_s} \nabla \Theta_s) - \gamma_{\Theta_s} + \phi_{gs} \quad \text{Eq. 5}$$

This partial differential equation was simplified to an algebraic equation by neglecting the convection and diffusion terms (7). The two final terms in Equation 5 are the collisional dissipation of energy (2) and the interphase exchange between the particle fluctuations and the gas phase (8). Solids stresses are calculated according to shear and bulk (2) viscosities. The shear viscosity consists of three parts: collisional (6, 8), kinetic (6) and frictional (9). The solids pressure formulation by Lun et al. (2) was enhanced by the frictional pressure formulation by Johnson and Jackson (10). The radial distribution function of Ogawa and Oshima (11) was employed.

Boundary conditions

A simple no-slip wall boundary condition was set for the gas phase. The Johnson and Jackson (10) boundary condition was used for the granular phase with a specularity coefficient of 0.25.

$$\bar{\tau}_s = -\frac{\pi}{6} \sqrt{3} \zeta \frac{\alpha_s}{\alpha_{s,\max}} \rho_s g_{0,ss} \sqrt{\Theta_s} \bar{U}_{s,\parallel} \quad \text{Eq. 6}$$

The inlet condition was specified as a velocity inlet injecting air at a flow rate of 0.6 m/s. CO2 was injected through a velocity inlet on the back wall to mimic the experiment. In the 2D simulation, CO2 was injected via a source term. The outlet was designated as a pressure outlet at atmospheric pressure.

Flow solver and solver settings

The commercial software package, FLUENT 13.0 was used as the flow solver. The phase coupled SIMPLE scheme (12) was used for pressure-velocity coupling and the higher order QUICK scheme (13) for the spatial discretization of all remaining equations. First order implicit temporal discretization was used (14).

Geometry and meshing

Both 2D and 3D geometries were completed on a 1.5x0.3 m² plan for 2D and a 1.5x0.3x0.015 m³ hexahedron for 3D. Meshing was done using a simple structured grid of completely square/cubic cells. A fine cell size of 2.5 mm (~5 particle diameters) was employed. The initial mesh consisted of 5 mm cells which were subsequently refined to 2.5 mm. Refinement was done by hanging node adaption only in the lower part of the domain where the bed material resides.

Initial conditions

The solution was initialized with zero velocity and no solids, after which solids were patched in at a volume fraction of 0.6 to the initial static bed height used in the experiment. The solution was run for 5 seconds in order to attain a quasi-steady flow condition. This solution was then used as the initial condition for time-averaging.

Simulation summary

A summary of the physical properties and simulation parameters are given in Table 1.

Table 1: Physical properties and simulation parameters

Gas density	1.225 kg/m ³
Gas viscosity	1.789x10 ⁻⁵ kg/m·s
Particle density	2500 kg/m ³
Particle size	500 μm
Bed dimensions	1.5x0.3 m ² (2D) & 1.5x0.3x0.015 m ³ (3D)
Particle-particle restitution	0.9
Specularity coefficient	0.25
Angle of internal friction	30°
Friction packing limit	0.50
Maximum packaging limit	0.63
Initial static bed height	0.4 m
Initial solids volume fraction	0.6

RESULTS AND DISCUSSIONS

Results will be presented by comparing tracer gas concentrations and particle velocity measurements between simulations and experiments. CO₂ tracer concentrations will be compared via cross-stream profiles at three heights: 10.5 cm, 34.5 cm and 60.5 cm. Solids velocity will be compared at 10 cm, 20 cm, 30 cm and 40 cm.

The tracer concentrations are compared in Figure 3a and 3b. It is immediately clear that the 2D simulation (Figure 3b) significantly under-predicts the tracer gas concentrations, while the 3D simulation gives a more reasonable comparison.

Two primary causes of the significant error in the 2D simulations can be identified: the friction at the front and back walls must be accounted for and the CO₂ concentration varies across the thickness of the bed (larger concentrations at the back wall where the tracer is injected and measured). These two effects will be discussed in some more detail.

2D simulations essentially assume a frictionless front and back wall, thereby allowing for simulated particle velocities which are much greater than experimental measurements (Figure 4). The implication of such over-predicted solids velocities on gas species transport is greater gas back-mixing (due to the stronger solids recirculation) and stronger convective mixing (due to the much larger amount of kinetic energy in the bed). These effects should cause more species diffusion, especially

towards the top of the bed. When comparing Figure 3a to Figure 3b this indeed appears to be the case.

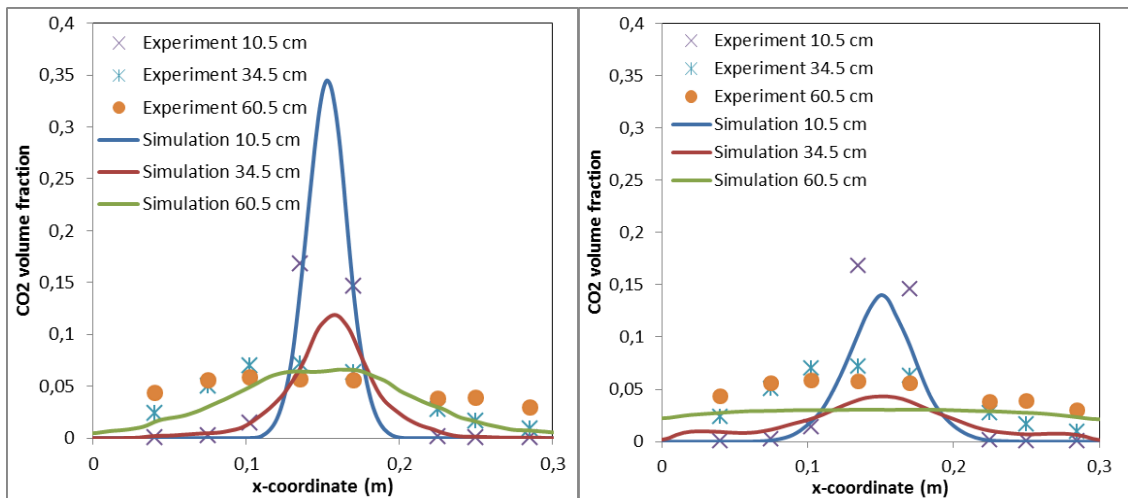


Figure 3: Comparison of cross-stream experimental and simulated CO_2 volume fraction profiles at different heights in the bed: a) (3D) case and b) (2D)

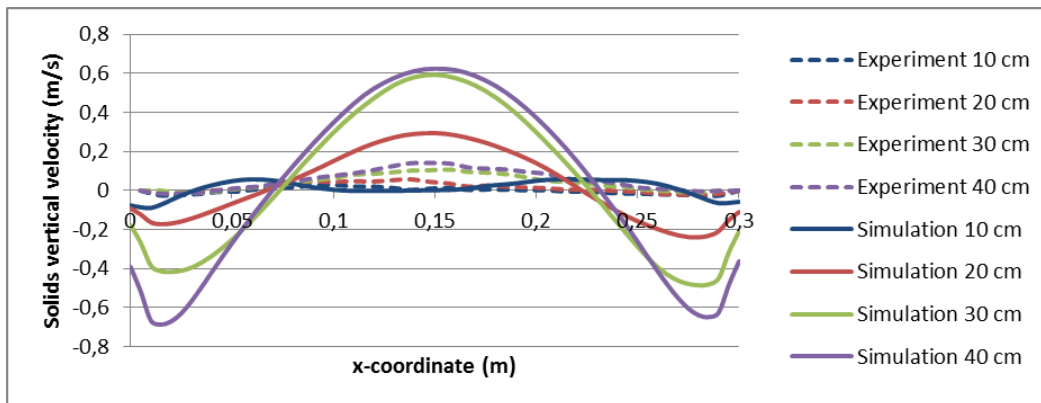


Figure 4: Comparison of cross-stream experimental and simulated (2D) solids vertical velocity profiles at different heights in the bed.

In order to explain the significant under-prediction of the tracer concentration by the 2D experiments, however, the second shortcoming of the 2D simulation must be considered: uniformity across the bed thickness. As shown in Figure 5, the tracer concentration varies significantly across the thickness of the bed with much higher concentrations occurring at the back wall than at the front. Since the 2D simulation essentially reports an average across the thickness and the 3D simulation reports the concentration at the back wall, the 3D simulation returns significantly higher tracer concentrations.

However, even though the 3D simulations predict tracer concentrations in the correct range, Figure 3a clearly indicates that not enough tracer diffusion occurs. The convective species transport should be captured with reasonable accuracy due to the much improved agreement with particle velocity measurements shown in Figure 6 (especially in the central regions where the tracer gas is injected). This implies that diffusive species transport is significantly under-predicted.

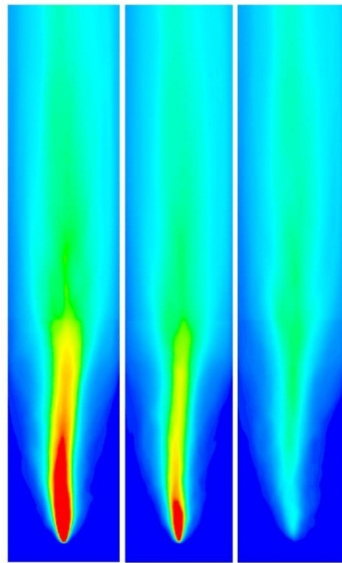


Figure 5: Tracer concentrations at the back wall (left), on a plane through the centre of the bed (middle) and at the front wall (right). The range is between 0 and 0.1 (CO₂ volume fraction).

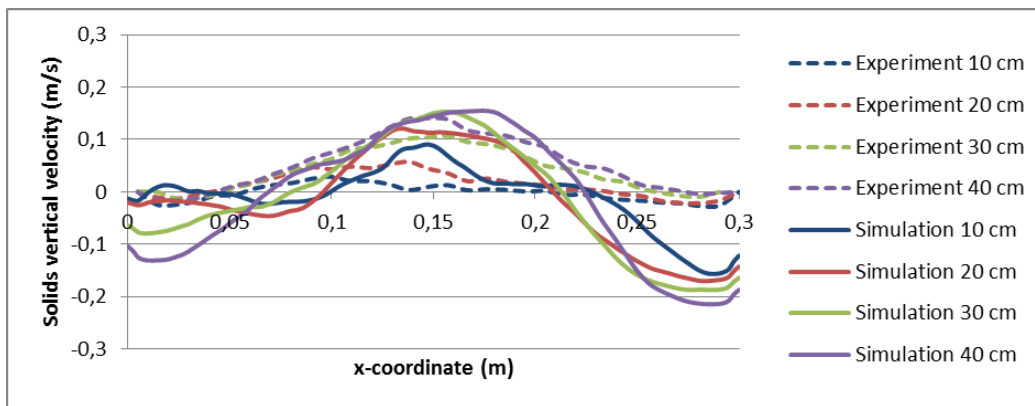


Figure 6: Comparison of cross-stream experimental and simulated (2D) solids vertical velocity profiles at different heights in the bed.

The data therefore suggests that additional modelling is required to account for particle-induced diffusion of gas species. This can be due to diffusion in the emulsion phase as shown in Figure 1 or perhaps also due to particle induced turbulence in regions with a lower solids volume fraction. Future work will derive the required particle-induced species diffusion model and test whether it has a significant impact on a reactive fluidized bed simulation.

Conclusions

Gas species transport was experimentally investigated in a pseudo-2D fluidize bed unit. Results were compared to 2D and 3D simulations to conclude that 3D simulations are mandatory for accurate prediction of the species transport. 2D simulations neglected wall friction on the front and back walls and did not capture the species gradient across the thickness of the bed.

3D simulations also showed that additional gas species diffusion modelling is required. Simulation data showed considerably less gas species diffusion than that which was recorded in the experiments and this was attributed to particle-induced diffusion of gas species which was not included in the simulation. Further work should be carried out in order to develop the necessary model and evaluate its impact on reactive fluidized bed simulations.

REFERENCES

1. Jenkins, J.T. and S.B. Savage, *Theory for the rapid flow of identical, smooth, nearly elastic, spherical particles*. Journal of Fluid Mechanics, 1983. **130**: p. 187-202.
2. Lun, C.K.K., S.B. Savage, D.J. Jeffrey, and N. Chepur, *Kinetic Theories for Granular Flow: Inelastic Particles in Couette Flow and Slightly Inelastic Particles in a General Flow Field*. Journal of Fluid Mechanics, 1984. **140**: p. 223-256.
3. Taghipour, F., N. Ellis, and C. Wong, *Experimental and computational study of gas-solid fluidized bed hydrodynamics*. Chemical Engineering Science, 2005. **60**(24): p. 6857-6867.
4. Ohno, K.-I., K. Nishioka, K. Munesue, T. Maeda, and M. Shimizu, *Diffusion behaviors of HE and CH4 in air flow through packed bed*. ISIJ International, 2012. **52**(8): p. 1389-1393.
5. Cloete, S., A. Zaabout, S.T. Johansen, M. van Sint Annaland, F. Gallucci, and S. Amini, *The generality of the standard 2D TFM approach in predicting bubbling fluidized bed hydrodynamics*. Powder Technology, 2013. **235**(0): p. 735-746.
6. Syamlal, M., W. Rogers, and T.J. O'Brien, *MFIX Documentation: Volume 1, Theory Guide*. 1993, Springfield: National Technical Information Service.
7. Van Wachem, B.G.M., J.C. Schouten, C.M. Van den Bleek, R. Krishna, and J.L. Sinclair, *Comparative analysis of CFD models of dense gas-solid systems*. AIChE Journal, 2001. **47**(5): p. 1035-1051.
8. Gidaspo, D., R. Bezburuah, and J. Ding, *Hydrodynamics of Circulating Fluidized Beds, Kinetic Theory Approach*, in *7th Engineering Foundation Conference on Fluidization* 1992. p. 75-82.
9. Schaeffer, D.G., *Instability in the Evolution Equations Describing Incompressible Granular Flow*. Journal of Differential Equations, 1987. **66**: p. 19-50.
10. Johnson, P.C. and R. Jackson, *Frictional-Collisional Constitutive Relations for Granular Materials, with Application to Plane Shearing*. Journal of Fluid Mechanics, 1987. **176**: p. 67-93.
11. Ogawa, S., A. Unemura, and N. Oshima, *On the Equation of Fully Fluidized Granular Materials*. Journal of Applied Mathematics and Physics, 1980. **31**: p. 483.
12. Patankar, S., *Numerical Heat Transfer and Fluid Flow*. 1980: Hemisphere Publishing Corporation.
13. Leonard, B.P. and S. Mokhtari. *ULTRA-SHARP Nonoscillatory Convection Schemes for High-Speed Steady Multidimensional Flow*. in *NASA TM 1-2568 (ICOMP-90-12)*. 1990. NASA Lewis Research Center.
14. Cloete, S., S. Amini, and S.T. Johansen, *On the effect of cluster resolution in riser flows on momentum and reaction kinetic interaction*. Powder Technology, 2011. **210**(1): p. 6-17.